Les Cahiers du GERAD ISSN: 0711–2440

A service-integrated hub-line location problem with demand elasticity and its application to the design of urban mobility hubs

B. Cobeña, C. Contardo

G–2025–11

January 2025

Citation suggérée : B. Cobeña, C. Contardo (Janvier 2025). A service-integrated hub-line location problem with demand elasticity and its application to the design of urban mobility hubs, Rapport technique, Les Cahiers du GERAD G– 2025–11, GERAD, HEC Montréal, Canada.

Avant de citer ce rapport technique, veuillez visiter notre site Web (https://www.gerad.ca/fr/papers/G-2025-11) afin de mettre à jour vos données de référence, s'il a été publié dans une revue scientifique.

Suggested citation: B. Cobeña, C. Contardo (January 2025). A service-integrated hub-line location problem with demand elasticity and its application to the design of urban mobility hubs, Technical report, Les Cahiers du GERAD G–2025–11, GERAD, HEC Montréal, Canada.

Before citing this technical report, please visit our website (https://www.gerad.ca/en/papers/G-2025-11) to update your reference data, if it has been published in a scientific journal.

La publication de ces rapports de recherche est rendue possible grâce au soutien de HEC Montréal, Polytechnique Montréal, Université McGill, Université du Québec à Montréal, ainsi que du Fonds de recherche du Québec – Nature et technologies.

Dépôt légal – Bibliothèque et Archives nationales du Québec, 2025
– Bibliothèque et Archives Canada, 2025

The publication of these research reports is made possible thanks to the support of HEC Montréal, Polytechnique Montréal, McGill University, Université du Québec à Montréal, as well as the Fonds de recherche du Québec – Nature et technologies.

Legal deposit – Bibliothèque et Archives nationales du Québec, 2025
– Library and Archives Canada, 2025

GERAD HEC Montréal
3000, chemin de la Côte-Sainte-Catherine
Montréal (Québec) Canada H3T 2A7

Tél. : 514 340-6053
Téléc. : 514 340-5665
info@gerad.ca
www.gerad.ca

A service-integrated hub-line location problem with demand elasticity and its application to the design of urban mobility hubs

Brenda Cobeña [a, b]

Claudio Contardo [a, b]

[a] *Department of Mechanical, Industrial and Aerospace Engineering, Concordia University, Montréal (Qc), Canada, H3G 1M8*

[b] *GERAD & CIRRELT, Montréal (Qc), Canada, H3T 1J4*

brenda.cobena@mail.concordia.ca

claudio.contardo@concordia.ca

January 2025
Les Cahiers du GERAD
G–2025–11

Abstract : This paper considers the problem of designing urban mobility hubs by modeling them as service-integrated hub-line location problems. We integrate traditional network design decisions (where to place and how to connect the mobility hubs) with microscopic decisions regarding the services to offer at each located hub. The proposed model assumes that demand is elastic not only to the travel times, but also to the services provided at the entrance/egress points in the network, therefore providing more sensitive and realistic modeling capabilities. The proposed model aims to maximize the overall time savings of the demand captured by the service-enhanced hub-line. We propose a mixed-integer programming model for this problem, where demand elasticity is incorporated via gravity models. We conduct a case study using a real transit network, namely that of the metropolitan City of Montreal, Canada. We show that the proposed framework leads in certain cases to hub-lines whose topologies cannot be derived from classical hub-line network design models, showcasing the relevance of integrating the service location decisions and demand elasticity to the enhanced service levels in the planning of a hub-line.

Keywords : Hub-line location, mobility hub, demand elasticity

Acknowledgements: We thank the Natural Sciences and Engineering Research Council of Canada (NSERC) for its financial support through Grants no. 2018–06704 and 2020–06311. We would like to extend our gratitude to Dr. Ivan Contreras for their constructive remarks in the early stages of this project.

1 Introduction

Urban transportation faces nowadays significant challenges, one of them due to the continuous increase in urban population and sprawl, resulting in longer commutes, increased traffic congestion, and negative environmental impacts (Schäfer, 2007; UN, 2009). Urban mobility hubs (UMHs) emerge as one of the solutions to create more efficient, accessible, and sustainable urban transportation networks to address these challenges. UMHs are strategic locations where different transportation modes converge. They facilitate seamless, sustainable travel and play a crucial role in urban transportation networks (Aydin et al., 2022).

UMHs can offer a variety of different services or amenities to the population. Some services may have a direct impact on the traveling times —think of bike sharing docks, for instance—, while others may have an indirect effect by attracting demand to the network —as is the case of grocery stores, or financial services. These hubs represent significant junctions where a substantial volume of journeys begin, end, or transition (Metrolink, 011b). Also, they act as convergence points for employment, housing, and recreation, rendering them significant economic and social activity centers (Arnold et al., 2023).

Significant advancements have been made in planning or implementing UMHs over the last few years. For instance, the city of Bremen in Germany integrates trams, buses, taxis, and bicycles. Edinburgh's mobility plan adds a layer of innovation by incorporating micro-hubs to manage last-mile deliveries. The city of Vienna integrates Mobility as a Service (MaaS) with public transit through its comprehensive mobility stations. In Portland, OR, the alignment of transit with land-use planning for growth areas showcases how cities use these hubs to enhance transportation efficiency. These precedents show how UMHs are becoming the backbone of the future of urban transportation, although their implementation remains a challenge. As UMHs evolve, they present a complex modeling and operational challenge, especially in the context of expanding urban transportation systems (Arnold et al., 2023).

The urban mobility hub network design is a challenging network design problem (NDPs), and Hub network location models have been implemented to enhance the mobility of passengers (see, Farahani et al., 2013; Alumur et al., 2021). These models address the location of special facilities—hubs— in the network, establishing connections between them. Hub facilities can be seen as transshipment nodes where there can be a change in the transport mode (e.g., bus stations and subway stations).

To maximize the attractiveness of UMHs, they should offer a range of services, such as car-sharing, bike-sharing, and access to points of interest (POIs) (Arnold et al., 2023). In this paper, we introduce a novel framework to the design of urban mobility systems as a hub line location problem (HLLP), incorporating demand elasticity into the optimization model, where in addition to optimizing location and connectivity, this study highlights the importance of incorporating service levels at hub locations, allowing for adjustments in response to demand elasticity.

This paper presents several significant contributions to the field of urban planning and optimization. The key contributions are as follows:

1. We introduce a novel modeling framework to the service-enhanced hub-line location problem with elastic demands (EDS-HLLP). This work extends our previous work (Cobeña et al., 2023) by considering additional decisions in the location of services at the located hubs, and their impact in the captured demands.
2. We present a mixed-integer programming formulation for the EDS-HLLP, and show that it can address small- to medium-sized problems.
3. We conduct a case study using data from the metropolitan area of Montreal to show the applicability of the proposed method in a real-world context of integrating service level of hubs, providing insights for city planners, urban planners and public transport managers on the design of urban mobility systems.

4. We provide evidence that the enriched modeling approach can lead to hub-lines with different topologies than to those that result from applying the earlier models that ignore the service location decisions, showcasing the relevance of integrating those decisions at a planning level and their impact in the demands.

The paper is structured as follows: Section 2 presents related literature and highlights the research gap we aim to address. Section 3 formally defines the considered problem setting and introduces our new gravity model to incorporate elasticity demand with level of services. Section 4 presents a path-based formulation. Section 5 present a case study area for the city of Montreal and extracts general insights for city or transport planners. We conclude with a summary and some remarks in section 6.

2 Literature review

Although research on mobility hubs has been growing lately, this field can still be qualified as a new research area. Recent studies have focused on providing a concept of what it is and how to classify them from urban context or their transportation role (see, Aono, 2019; Arnold et al., 2023; SANDAG, 2017). From an optimization planning model perspective, current research focuses on optimizing hub locations decisions to improve the efficiency of the transportation networks. For instance, Nair and Miller-Hooks (2014) propose an equilibrium network design model that integrates the optimal location for shared-vehicle stations into the city's metro network. Similarly, Steiner and Irnich (2020) introduce a network planning optimization model for bus lines that integrate inter-modal trips with ride-sharing mobility modes used as a first or last leg. Caggiani et al. (2020) propose a model that promotes using bike-sharing systems (BSS) as a feeder mode for public transport, focusing on improving accessibility and promoting social equality.

Recently, Frank et al. (2021) proposed two models to optimize hub locations in rural areas, one aiming at improving the accessibility to POIs, and the second to improving workplace accessibility. Xanthopoulos et al. (2024) proposed a model to optimize the location and capacity of mobility hubs to maximize the total utility experienced by individuals traveling using traditional and/or shared modes. Stadnichuk et al. (2024) introduced optimization models to determine the optimal locations for mobility hubs.

In the context of network design problems, hub location problems (HLP) have been extensively studied to optimize the location of hubs in a transportation network (Alumur et al., 2021). Particularly, the hub-line location Problem (HLLP) highlights the importance of designing a corridor (e.g. subway line or a rapid transit bus corridor) to improve passenger mobility in their daily trips. Martins de Sá et al. (2015) were the first to introduce the HLLP, which consists of determining the optimal location of hubs and connecting them using a line, to minimize the total travel time for passengers. The HLLP approach is helpful, especially in areas with high demand for interconnected transport services, such as those commonly found in large metropolitan areas, providing a foundation for designing urban mobility hubs. The demand in HLLPs is assumed to be an exogenous input to the problem of designing the hub line network; however, this may not be a reasonable assumption. According to Alumur et al. (2021), the nature of the demand and how it affects the resulting hub network is a key aspect for a better modeling of HLPs. The same authors highlight the importance of incorporating demand elasticity to prices or quality of service.

Facility location problems with demand elasticity have already been the subject of study in the recent literature. For instance, Drezner and Drezner (2001) were the first to employ a gravity model to incorporate elastic demands in hub location models. Moreover, Eiselt and Marianov (2009) studied the HLPs under competitive situations to maximize the total market share where gravitational models define the user's choice. Several studies consider modeling or solving facility location problems with elastic demands, as in Eiselt and Laporte (1998); Laporte et al. (2002); Drezner and Drezner (2002, 2004, 2006, 2007) and Erdoğan et al. (2010), where demand elasticity is modeled through gravity models. In network design problems, Zetina et al. (2019) introduced the profit-oriented multi-commodity network design with elastic demand. These studies highlight the importance of incorporating demand elasticity, especially in hub-location problems arising in public transportation.

The most recent advances in HLLPs is the *profit-oriented hub line location problem with elastic demand* (ED-HLLP) introduced by Cobeña et al. (2023). This problem seeks to maximize the profit that, in turn, depends on the time savings obtained when using the hub-line system with respect to the existing network. The authors use gravity models to incorporate demand elasticity into an optimization model. In Cobeña and Contardo (2024) the authors build upon the previous work to propose a column generation heuristic for the problem, being able to tackle larger problems.

Despite these advances, there still is a lack in understanding the integration of demand elasticity when designing hub-line public transit networks. To address this issue, we propose a new framework inspired by ED-HLLP model for designing urban mobility hubs; it is denoted as *service-enhanced profit-oriented hub line location problem with elastic demand* (EDS-HLLP). This new model introduces an objective function based on gravity models to include demand elasticity, offering different levels of services in the access/egress to mobility hubs to maximize the overall profit by reducing travel times when using the hub-line system with respect to the existing network.

3 Problem definition

In this section we introduce the notation and provide the problem definition for the EDS-HLLP. We divide this section in four sub-sections. In Section 3.1 we introduce the parameters and network representation of the EDS-HLLP. In Section 3.2 we introduce the notation used to identify the possible service offering at the potential hub sites. In Section 3.3 we present our choice for modeling demand elasticity by combining demand and gravity models, giving raise to the objective function considered in our study.

3.1 Preliminaries

We adopt in this section the same notation used in Cobeña et al. (2023); Cobeña and Contardo (2024) for the ED-HLLP, and extend it to the EDS-HLLP. The problem is defined on a directed graph $\widetilde{G} = (N, A)$ derived from the undirected graph $G = (N, E)$ where N is the set of nodes and E the set of edges $e := [k, m]$ with $k < m$. Here $A = \{(k, m) \cup (m, k) : e = [k, m] \in E\}$ is the set of arcs induced by E. Hub nodes or facilities can be seen as central stations such as subway, tram, bus or train stations and non-hubs correspond to bus stops, taxi stations, or urban areas. The commodity $c \in C$ represents the collection of OD pairs whose demands must be routed either through a hub line or directly from origin to destination, and its origin and destination nodes are denoted o_c and d_c, respectively.

For each commodity $c \in C$, $t_{o_c d_c} \geq 0$ represent the optimal (minimum) travel time required to travel from o_c to d_c in the absence of the hub line. Without loss of generality, $t_{o_c d_c}$ also incorporates any average transfer time required when changing modes of transportation from o_c to d_c. When a hub arc is located between hub nodes $(k, m) \in A$, the travel time between k and m is computed as $\alpha_{km} t_{ij}$, where $0 \leq \alpha_{km} \leq 1$ represents a reduction factor that models the use of a faster transport technology to connect o_c and d_c. Also, the access and exit times to the hub line through node $i \in N$ respectively are incorporated, denoted as $\tilde{t}_i^a \geq 0$ and $\tilde{t}_i^e \geq 0$ respectively.

One remarkable extension that we now make to the earlier model of Cobeña et al. (2023) is the consideration of conflict constraints. In the proposed model, we assume the existence of a set $I \subseteq A \times A$ such that, for every tuple $(a, b) \in I$, the model can select at most one of these arcs to be part of the optimal hub-line. This constraint is relevant in situations where design considerations prevent pairs of arcs to be selected simultaneously, for instance in subway lines when such arcs cross, potentially leading to more challenging engineering designs.

3.2 Modeling the service offerings at the hub nodes

Let us define some notations related to offering different services at the potential hub-nodes. Let us denote $\mathcal{S}$, the set of all possible services. For every potential hub location k we let $\mathcal{S}(k) = \{s_1^k, s_2^k, \ldots, s_l^k\} \subseteq 2^{\mathcal{S}}$ be the set of potential subsets of services that may be offered at site k. The definition of $\mathcal{S}(k)$ is sufficiently general so it can capture several possible cases relevant in practice:

1. If each service $s \in \mathcal{S}$ occupies a certain space (in m^2 for instance) that we denote q_s, and Q_k denotes the total available space at location k (in the same units), then $\mathcal{S}(k)$ could be defined as $\mathcal{S}(k) = \{S \subseteq \mathcal{S} : \sum\{q_s : s \in S\} \leq Q_k\}$.
2. If the infrastructure associated with each service $s \in \mathcal{S}$ has a cost (in \$ for instance) that we denote c_s, and B_k denotes the total budget available for locating infrastructure at location k, then $\mathcal{S}(k)$ could be defined as $\mathcal{S}(k) = \{S \subseteq \mathcal{S} : \sum\{c_s : s \in S\} \leq B_k\}$.
3. If each service $s \in \mathcal{S}$ is associated with a cost c_s and a space q_s, and there are budget and space availabilities at node k denoted B_k, Q_k, the set $\mathcal{S}(k)$ could be defined as $\mathcal{S}(k) = \{S \subseteq \mathcal{S} : \sum\{c_s : s \in S\} \leq B_k, \sum\{q_s : s \in S\} \leq Q_k\}$.

In addition to the individual budget constraints that model the limits in space and budget for installing services at each individual hub-node, we also assume the existence of a global budget B (in units of space, money, or other), and let $\mathcal{C}_{ks}$ be the consumption of that budget for a subset of services $s \in \mathcal{S}_k$ at the hub-node k.

3.3 Service-dependent demand elasticity

We next present the objective function of the problem, inspired from the work of Sonesson (2001). Let us assume that the attractiveness associated to a commodity c, and denoted $F(A_c)$, depends linearly on the set of services available at the entrance and egress locations to/from the system. For every $k \in N$ we let h_k^o, h_k^d be binary indicators equal to 1 if k is the entrance/egress hub for commodity c. For every service $s \in \mathcal{S}$ and potential hub-node $k \in N$, we let α_{ks}, β_{ks} be the marginal attractiveness provided by the presence of a service s at the entrance/egress location k. We can express $F(A_c)$ now as follows:

$$F(A_c) = \alpha_c + \sum_{k \in N} \sum_{s \in \mathcal{S}} \left(h_k^o \alpha_{sk} + h_k^d \beta_{sk} \right), \tag{1}$$

where α_c represents the revenue R_c for each unit of time reduction associated with the commodity c multiplied by the size of the populations $P_{o_c} P_{d_c}$. Note that this linear model assumes that the services at the intermediate hub nodes have no effect on the demand associated to commodity c. This assumption is relevant in contexts where the user typically does not interact with the services available at the intermediate hub nodes, which is typically the case of multiple subway systems.

Our optimization model —to be described in the next section— assumes that the total demand captured, and the corresponding time savings, are known at the level of the variables definition. This means that, in addition to the information regarding entrance/egress nodes, the subsets of services available at each one of them must be incorporated at the variable definition level. A path π is therefore defined as the following tuple:

$$\pi = [o_c, (h_1, s_1), h_2, \ldots, h_{k-1}, (h_k, s_k), d_c]. \tag{2}$$

The nodes o_c, d_c represent the origin/destination nodes of commodity c, which may or may be not coincide with potential hub locations. The sequence $(h_1, \ldots, h_k)$ corresponds to the sequence of hubs taken by the commodity c. Finally, $s_1 \in \mathcal{S}(h_1), s_k \in \mathcal{S}(h_k)$ correspond to the subsets of services available at the entrance/egress points. This new definition of π allows different hubs to offer different combinations of services, providing more flexibility in routing and service utilization. Following Cobeña et al. (2023)'s nomenclature, we can further categorize paths $\pi \in \mathcal{P}_c$ as follows:

($\mathbf{ODH}_c$)-paths. Corresponding to paths in which all the nodes are hubs. In particular, o_c and d_c must be hubs.

($\mathbf{DH}_c$)-paths. these paths mean that the origin node (o_c) is not a hub node but the destination node (d_c).

($\mathbf{OH}_c$)-paths. Corresponding to paths whose destination node (d_c) is not a hub node, but the origin node (o_c) is.

($\mathbf{ODNH}_c$)-paths. Corresponding to paths in which neither o_c nor d_c are hub nodes.

Moreover, for two subsets of services $s_1, s_k \in 2^{\mathcal{S}}$ we let $T_{cs_1s_k}$ be the set of paths that benefit from services s_1, s_k at the entrance/egress from the system, for $T \in \{\text{ODH}, \text{DH}, \text{OH}, \text{ODNH}\}$. We also further denote $T_{c\cdot s_k} = \cup\{T_{c\tau s_k} : \tau \in 2^{\mathcal{S}}\}$, and $T_{cs_1\cdot} = \cup\{T_{cs_1\tau} : \tau \in 2^{\mathcal{S}}\}$, for $T \in \{\text{ODH}, \text{DH}, \text{OH}, \text{ODNH}\}$.

Note that for some paths where the origin or destination are hubs, we have that $h_1 = o_c$ or $h_k = d_c$. Finally, the travel time for routing commodity $c \in C$ via path $\pi \in \mathcal{P}_c$ ($\tau_{\pi c}$) is defined as a Cobeña et al. (2023) proposed:

$$\tau_{\pi c} = t_{o_c h_1} + \tilde{t}^a_{h_1} + \sum_{m=1}^{k-1} \alpha t_{h_m h_{m+1}} + \tilde{t}^e_{h_k} + t_{h_k d_c}. \tag{3}$$

With the new path definition, we reformulate $F(A_c)$ as $F(A_{\pi c})$ to reflect the different combinations of services available for each commodity and type of path π. The demand associated to a path $\pi = (o_c, (h_1, s_1), h_2, \ldots, h_{k-1}, (h_k, s_k), d_c)$ for a commodity c is denoted $F(A_{\pi c})$ and defined as follows:

$$F(A_{\pi c}) = \alpha_c + \sum_{s \in s_1} \alpha_{s h_1} + \sum_{s \in s_k} \beta_{s h_k}. \tag{4}$$

The Equation (4) represents the *attractiveness function* $F(A_{\pi c})$ for a given path π and commodity c, incorporating the effect of different combinations of services offered at the hubs. The terms appearing in this equation correspond to those appearing in Equation (1) for the fixed sets of services s_1, s_k associated to the path π.

Finally, we define the final demand (w_c) of a commodity c, as follows:

$$w_c = \frac{F(A_{\pi c})}{\tau^r_{\pi c}} \tag{5}$$

This leads to the following terms in the objective function for the *service-enhanced profit-oriented hub line location problem with elastic demand* (EDS-HLLP):

$$g_{\pi c} = \frac{F(A_{\pi c})}{\tau^r_{\pi c}}(t_{o_c d_c} - \tau_{\pi c}) \tag{6}$$

We are now in a position to introduce the mathematical model for the EDS-HLLP.

4 Mathematical formulation for the EDS-HLLP

In this section we introduce a mathematical formulation for the EDS-HLLP. The proposed model leverages the fact, that, if the travel times ($\tau_{\pi c}$) are known a priori, the objective function (6) becomes linear. Therefore, travel times are precomputed for every $\pi \in \mathcal{P}_c$, for every commodity $c \in C$.

In order to do this, we need to define the following family of variables: the binary hub-line variables $v_{\pi c}$, $\pi \in \mathcal{P}_c, c \in C$, equal to 1 if and only if commodity c is delivered using path π. Also, we let z_{ks} be equal to 1 if and only if a hub is located at node k and the subset of services $s \in \mathcal{S}(k)$ offered at it. We let $y_{km}, (k,m) \in A$ be equal to 1 if and only if a hub arc is located between hubs k and m, enabling flows to be routed in both directions. Furthermore, we implement the sub-tour elimination constraints for the arc variables y using an additional set of variables l_k for every hub-node k representing the order in which node k appears in the hub line. Besides the variable set, we also make use of parameters $h_e^{\pi c}$ equal to 1 if and only if path $\pi \in \mathcal{P}_c$ contains the arc (k,m) or (m,k) defined by edge $e = [k,m] \in E$. The EDS-HLLP can be modeled as the following MILP, that we denote (P_1):

$$\max \quad \sum_{c \in C} \sum_{\pi \in \mathcal{P}_c} g_{\pi c} v_{\pi c} \tag{7}$$

$$\sum_{k \in N} \sum_{s \in \mathcal{S}(k)} z_{k,s} = p, \tag{8}$$

$$\sum_{k \in N} \sum_{\substack{m \in N \\ (k,m) \in A}} y_{km} = p - 1, \tag{9}$$

$$\sum_{s \in \mathcal{S}(k)} z_{ks} \leq 1, \qquad k \in N, \tag{10}$$

$$\sum_{k \in N} \sum_{s \in \mathcal{S}(k)} z_{ks} \mathcal{C}_{ks} \leq B, \tag{11}$$

$$\sum_{\substack{m \in N \\ (k,m) \in A}} y_{km} + \sum_{\substack{m \in N \\ (m,k) \in A}} y_{mk} \leq 2 \sum_{s \in \mathcal{S}(k)} z_{ks}, \qquad k \in N \tag{12}$$

$$\sum_{\substack{l \in N \\ (k,l) \in A}} y_{kl} \geq \sum_{s \in \mathcal{S}(k)} z_{ks} + \sum_{s \in \mathcal{S}(m)} z_{ms} - 1, \qquad k, m \in N, k < m, \tag{13}$$

$$l_k - l_m + n y_{km} \leq n - 1, \qquad (k,m) \in A, \tag{14}$$

$$y_{ij} + y_{kl} \leq 1, \qquad \forall (i,j), (k,l) \in I, \tag{15}$$

$$\sum_{\pi \in \mathcal{P}_c} h_{[k,m]}^{\pi c} v_{\pi c} \leq y_{km} + y_{mk}, \qquad [k,m] \in E, c \in C, \tag{16}$$

$$\sum_{\pi \in \mathcal{P}_c} v_{\pi c} \leq 1, \qquad c \in C, \tag{17}$$

$$\sum_{\pi \in (\mathrm{ODH}_{c \cdot s})\text{-paths}} v_{\pi c} + \sum_{\pi \in (\mathrm{DH}_{c \cdot s})\text{-paths}} v_{\pi c} \leq z_{d_c s}, \qquad c \in C, s \in \mathcal{S}(d_c), \tag{18}$$

$$\sum_{\pi \in (\mathrm{ODH}_{cs \cdot})\text{-paths}} v_{\pi c} + \sum_{\pi \in (\mathrm{OH}_{cs \cdot})\text{-paths}} v_{\pi c} \leq z_{o_c s}, \qquad c \in C, s \in \mathcal{S}(o_c), \tag{19}$$

$$y_{km} \in \{0,1\}, \qquad k, m \in N, (k,m) \in A \tag{20}$$

$$z_{ks} \in \{0,1\}, \qquad k \in N, s \in \mathcal{S}(k), \tag{21}$$

$$v_{\pi c} \in \{0,1\}, \qquad c \in C, \pi \in \mathcal{P}_c. \tag{22}$$

The proposed model aims to maximize the profit (7) that, in turn, depends on the time savings obtained when using the hub-line system as well as the demand captured given the services provided at the hub line's access and egress nodes.

Constraints (8) and (9) strictly define the number of hubs with offered service and inter-hub links to be installed. Constraints (10) is to avoid overlaps in the set of services and to guarantee that no more than one set of services can be installed on a hub. Constraint (11) limits the total expenses for the installation of services to B. The series of constraints from (12) through (14) are crafted to uphold the design of the hub-line. Specifically, constraints (12) limit each hub to a maximum of two links to other hubs, while constraints (13) dictate that there must be at least one outgoing arc from each hub node on the path, excluding the hub node with the largest index to mitigate the appearance of symmetric solutions. The constraints (14), also referred to as Miller-Tucker-Zemlin (MTZ) constraints, act as sub-tour elimination constraints (SECs), ensuring uninterrupted connectivity of the hub-line. Also, constraints (15) are introduced to prevent the model from selecting incompatible hub arcs. Furthermore, constraints (17) restrict that each commodity is transported using the hub line, and constraints (16) enforce the exclusive use of paths where hub arcs are opened. The constraints (18) and (19) ensure that the use of paths of types ODH_c, DH_c, and OH_c is consistent with the services offered in the respective entrance/egress nodes. The decision variables domain is defined by constraints (20)–(22).

4.1 Solving the path-based formulation for the EDS-HLLP

The MILP formulation proposed in the previous section uses the candidate OD paths of each commodity as an input. In this work, we adapt the mathematical procedure proposed by Cobeña et al. (2023) to enumerate all candidate paths. Remarkably, we use Cobeña et al. (2023)'s enumeration method to enumerate *partial paths* of the form $\pi' = (o_c, h_1, \ldots, h_k, d_c)$, this is without considering the services available at the entrance/egress nodes. For each such partial path π' we consider all possible combinations of paths $\pi = (o_c, (h_1, s_1), h_2, \ldots, h_{k-1}, (h_k, s_k), d_c)$ for all possible tuples $(s_1, s_k) \in \mathcal{S}(h_1) \times \mathcal{S}(h_k)$. The objective term $g_{\pi c}$ is then computed according to formula (6) for every resulting path π.

4.1.1 Solution algorithm

We now describe in full detail the enumeration procedure used to construct feasible paths $\pi \in \mathcal{P}_c$ for $c \in C$.

Step 1 (Initialization). We construct a graph $G = (N, E)$, where N represents the set of demand points and potential hub locations, and E denotes the set of edges connecting these points. The travel time required to traverse edge $e = [i, j] \in E$ is denoted by t_{ij}.

Step 2 (Calculation of travel times). For each commodity $c \in C$, an auxiliary graph $G_c = (N_c, A_c)$ is constructed and the travel times t^c are calculated by applying the path generation procedure proposed by Cobeña et al. (2023). Further details can be found in Appendix A.

Step 3 (Partial path generation). With the auxiliary graph $G_c = (N_c, A_c)$ and the travel times t^c, all possible partial paths with a number of arcs less than or equal to $p + 1$ (where p is the number of open hubs) are identified. The *all_simple_paths* function from the *Networkx* library in Python is used for this purpose. For further details of the proposed procedure by Cobeña et al. (2023), refer to Appendix B.

Step 4 (Generation of full paths). Once all valid partial paths are generated in the previous step, a post-processing step is performed to account for the different combinations of services available at the access hub h_1 and the exit hub h_k. For each partial path $\pi' = (o_c, h_1, \ldots, h_k, d_c)$ generated in the previous step, we iterate through all possible combinations of services $(s_1, s_k) \in \mathcal{S}(h_1) \times \mathcal{S}(h_k)$.

Step 5 (Calculation of profits). For each path $\pi \in \mathcal{P}_c$ and its associated combinations of services, calculate the profit $g_{\pi c}$ using Equation (6).

Step 6 (Solve the MILP). Use the paths enumerated to feed problem (7)–(22) and solve it using a commercial solver.

5 Case study: determining an urban mobility hub line system in Montreal

In this section we assess the effectiveness of our proposed model, both in terms of its computational performance, as well as in terms of the quality of the solutions obtained. The mathematical model serves as a decision support tool for identifying hubs that provide services and facilitate connections among them, forming a Hub Line Network. The proposed model can be effectively implemented at a fine-grained level when comprehensive data is available. However, this study is constrained to neighbourhood-level data. Despite this limitation, the model remains a valuable resource for decision-makers. To evaluate the methodology, we utilize a real dataset from the metropolitan area of Montreal. The detailed analysis is based on instances derived from the Montreal OD survey (for further details, see Cobeña et al. (2023)).

The algorithm has been implemented in Python v3.9.14, and IBM CPLEX 22.1.1 has been used to solve the linear and integer programs associated with our approach. All experiments were conducted on an Intel Xeon Gold 6258R CPU @ 2.70GHz with a 512GB RAM computer with a time limit set to 24 hours. Additionally, to generate all candidate paths between OD pairs, as proposed in Cobeña et al. (2023), the maximum number of simultaneous sub-processes was limited to 4 CPUs.

5.1 Parameters

In this section, we specify the different parameters used in our experiments. The parameters related to services offered at the location of the hubs are denoted as service 1, 2 . . ., s. According to the literature, the most frequent services offered in a mobility hub are shared services such as shared bikes or cars, and important POIs, where these can be located near public transportation such as rapid transit network (Xanthopoulos et al., 2024; Arnold et al., 2023). This strategy offers adaptability, flexibility and the opportunity to make necessary tuning of parameters, evaluate the impact of the configuration on the resulting hub line network and the trade-off between maximizing profits, travel time savings and spatial coverage, to meet the needs of citizens.

Regarding the choice of the problem parameters, we use $R_c = (1 + \gamma_c)t_{o_c d_c}$ withγ_c drawn from an uniform distribution in $[0, 1]$, $r = 2.68$ (see, Goh et al., 2012). We make use of the same set of instances used in Cobeña et al. (2023), with $\alpha \in \{0.2, 0.5, 0.8\}$ and $p \in \{5, 7\}$. Similarly to Martins de Sá et al. (2015), we assume that access and egress times to/from the network are independent of the nodes, i.e., $\tilde{t}^a_k = \tilde{t}^a$ and $\tilde{t}^e_k = \tilde{t}^e$ for all $k \in N$. Additionally, the access and exit times are defined as a proportion of the average travel time:

$$\tilde{t}^a = \tilde{t}^e = \vartheta \frac{\sum_{(i,j)\in A} t_{ij}}{n \cdot (n-1)}, \tag{23}$$

where ϑ is fixed to 0.1 for our computational campaign.

Regarding the weights α_i and β_i associated with the second and third terms in Equation (4) —which account for the services at the access and exit hubs— are drawn from an uniform distribution in the interval $(0, 1]$, therefore ensuring that all weights are greater than zero. Since the three components in Equation 4 are measured in different units, a scaling factor τ is incorporated in the second and third terms.

Regarding the maximum number of service parameter B, in the analysis in Section 5.2 and 5.3, we define three different values: $B_1 = p * s$, $B_2 = 2/3(p * s)$ and $B_3 = 1/3(p * s)$ for $s = 3$ and $p = 5, 7$.

Finally, we consider incompatibility constraints I including all pairs of crossing arcs. We consider the geographical coordinates of the nodes, and the straight segments between them to populate the pairs of arcs that cross in the map.

5.2 Computational sensitivity analysis to the parameters r, p, α, and B

In this section, we conduct a computational sensitivity analysis of the proposed optimization method using a test-bed of 108 instances derived from the different values of B parameter described in Section 5.1 to analyze how the parameters r, p, α, and B affect the computational times. Each row from Tables 1–4 presents the average, aggregated by r, p , α and B parameters. Column *#Opt* show the number of optimal solutions found within 86400 seconds (1 day) of CPU time, the average of paths is displayed in column $\mid \mathcal{P} \mid$, column (t_{paths}) indicates the average CPU time spent in the enumeration of the partial paths, this is the paths that ignore the provided services at the hub locations t_{paths}, column (t_{post}) indicates the average CPU time spent in the enumeration of the full paths, this is the paths that include the services at the entrance/egress points in each case. Column (t_{MIP}) indicates the average CPU time spent in solving the MILP (7)–(22) to optimality, column (t_{tot}) corresponds to the average of the sum of all the times. See Appendix C to see the detailed results on Tables 8–10.

In this analysis the average used is geometric mean. For a collection $X = \{x_1, \ldots, x_n\}$ of n real numbers (not necessarily unique), the geometric mean is defined as:

$$gm(X) = \sqrt[n]{\prod_{i=1}^{n} x_i}.$$

Furthermore, we consider geometric means for all the averages reported, except for the average computing times that are reported using a shifted geometric mean with shift value $t = 1.0$. The shifted geometric mean that, for X and a shift value $t \in \mathbb{R}$, is defined as:

$$gm(X,t) = \sqrt[n]{\prod_{i=1}^{n} (x_i + t)} - t.$$

5.2.1 Effect of parameter n

From the results reported in Table 1, we can observe that the number of paths ($\mid \mathcal{P} \mid$) increases and the number of solved instances decrease as n increases. For instance for small instances most of them are solved optimally. Also, the computational times generally increases with n. However, the model remains computationally tractable even for some large instances, with three out of 18 problems being solved within the maximum time for $n = 39$.

Table 1: Computational sensitivity for different values of parameter n

n	#Opt	$\mid \mathcal{P} \mid$	t_{paths}	t_{post}	t_{MIP}	t_{tot}
10	16/18	74547	2.43	4.25	163.72	195.55
15	12/18	35350	56.70	1.07	43.90	148.01
20	12/18	79982	562.94	3.08	363.59	1838.99
25	9/18	121337	1425.52	7.38	433.94	5177.82
30	6/18	435481	978.15	25.18	1434.63	4191.23
39	3/18	90112	2090.89	15.57	111.55	2338.09

5.2.2 Effect of parameter p

Table 2 presents the computational sensitivity for the different hubs values (p). For instance, when $p = 5$, 36 out of 54 instances are solved optimally; however, when $p = 7$, the problem becomes more challenging, dropping to 22 solved instances. Regarding the computational times to solve the problem, it increases as p increases.

Table 2: Computational sensitivity for different values of parameter p

p	#Opt	$\mid \mathcal{P} \mid$	t_{paths}	t_{post}	t_{MIP}	t_{tot}
5	36/54	97535	41.35	5.59	147.56	325.48
7	22/54	66453	283.63	3.16	315.01	1990.11

5.2.3 Effect of parameter α

Table 3 shows the impact of parameter α, which represents the discount factor $(1-\alpha)$ for the use of the hub-line system. We observe that low discount factors ($\alpha = 0.8$) lead to easier problems, whereas the opposite occurs for high discount factors as α decreases. This can be explained by the ability of the path enumeration method to discard paths that do not represent any time savings for the passengers. In this situation, our method enumerates a lesser number of paths, which results in smaller and easier MILPs.

Table 3: Computational sensitivity for different values of parameter α

α	**#Opt**	$\lvert \mathcal{P} \rvert$	t_{paths}	t_{post}	t_{MIP}	t_{tot}
0.2	4/36	3044751	4.89	57.38	15405.19	15771.35
0.5	24/36	255230	139.60	5.80	821.13	1328.42
0.8	30/36	14057	127.72	1.59	22.25	195.47

5.2.4 Effect of parameter B

Table 4 shows the effect of parameter B; it refers to the total allocated budget for the location of services. The different values of B are the as defined in Section 5.1. We can observe that, in general terms, the CPU time required to solve the MILPs increases as the value of B decreases, possibly due to the larger combinatorial spectrum of choices relative to the location of fewer services across all hub-nodes.

Table 4: Computational sensitivity for different values of parameter B

B	**#Opt**	$\lvert \mathcal{P} \rvert$	t_{paths}	t_{post}	t_{MIP}	t_{tot}
$B = p * s$	20/36	78774	102.10	4.33	49.62	336.50
$B = \frac{2}{3}(p * s)$	19/36	94234	84.80	5.07	398.19	983.76
$B = \frac{1}{3}(p * s)$	19/36	76850	93.36	3.94	433.75	1036.73

5.3 Managerial insights

In this section we present several sensitivity analyses to assess the behavior of the proposed hub-line plans to variations of several parameters. The analyses are restricted to the problems for which our algorithm did not run out of resources. We also compare the plans obtained by the proposed method against those that would be obtained by the earlier method of Cobeña et al. (2023) that does not integrate the demand elasticity to the services offered into account. We remark that the proposed analyses align with the focus often encountered in the urban mobility literature (Xanthopoulos et al., 2024).

5.3.1 Demand captured and time savings

Tables 5–7 provide comparisons between the plans provided by the proposed model and those of the earlier work of Cobeña et al. (2023), which do not account for the demand elasticity to the services provided at the hub nodes. These comparisons are performed based on two main indicators: the % of served demand and % of total time savings. Our results show that the new model (under the column *EDS-HLLP*) is capable of producing solutions that typically capture higher demands, however, while providing lower time savings, especially when we focus on lower values of the parameter α (0.2 and to a lower extent also 0.5).

However, the average time savings tend to decrease when services are offered at the hubs. This counterintuitive behavior can be explained by the implicit trade-off between the time savings and the demand captured by the demand model. Look, for instance, to the results obtained with $\alpha = 0.5$ in

Table 7, where the served demand increases from 15% (when the elasticity to the services provided is ignored) to a 30% thanks to the increased demand, while the time savings suffer a reduction from 25% to 17%.

Table 5: ED-HLLP vs EDS-HLLP by parameter n

n	ED-HLLP		EDS-HLLP	
	% served demand	% saved time	% served demand	% saved time
10	27%	17%	35%	14%
15	12%	15%	13%	10%
20	9%	15%	8%	9%
25	3%	9%	4%	7%
30	3%	11%	5%	8%
39	1%	4%	1%	4%

In the same line of analysis, we observe that the time savings and percentages of captured demand tend to decrease as n increases, as per the results reported in Table 5.

Table 6: ED-HLLP vs EDS-HLLP by parameter p

p	ED-HLLP		EDS-HLLP	
	% served demand	% saved time	% served demand	% saved time
5	9%	14%	9%	10%
7	10%	13%	16%	10%

Table 7: ED-HLLP vs EDS-HLLP by parameter α

α	ED-HLLP		EDS-HLLP	
	% served demand	% saved time	% served demand	% saved time
0.2	73%	33%	87%	35%
0.5	15%	25%	30%	17%
0.8	2%	5%	3%	4%

5.3.2 Impact of locating services

Figure 1 shows the improvement in accessibility when the number of services (s) increases. For this analysis we assume that $B = ps$, which in practice means that every selected hub can allocate up to s services. For instance, when $s = 0$ using the model proposed by Cobeña et al. (2023), the percentage of served demand is lower than incorporating different service levels. Although we observe is a slight increase on the average total travel times for the users, the trade-off provided by the additional attractiveness provides a better coverage (in terms of the total demand captured), making it more accessible, while still providing positive savings.

5.3.3 Effect of adding services for different hub line configurations

Next, we analyze the impact of service integration for different values p. For this analysis we assume that $s = 3$ and that $B = ps$. We compare the proposed model against ED-HLLP of Cobeña et al. (2023). Figure 2 shows the effect of p on the percentage of served demand; we can see how the proposed model provides a higher coverage than the earlier model. The differences become more pronounced as the number of hubs increases. This reflects the observation that adding services triggers the attraction of more users to the hub line system, which in turn highlights the importance of integrating the planning of services within the problem of designing the hub-line network.

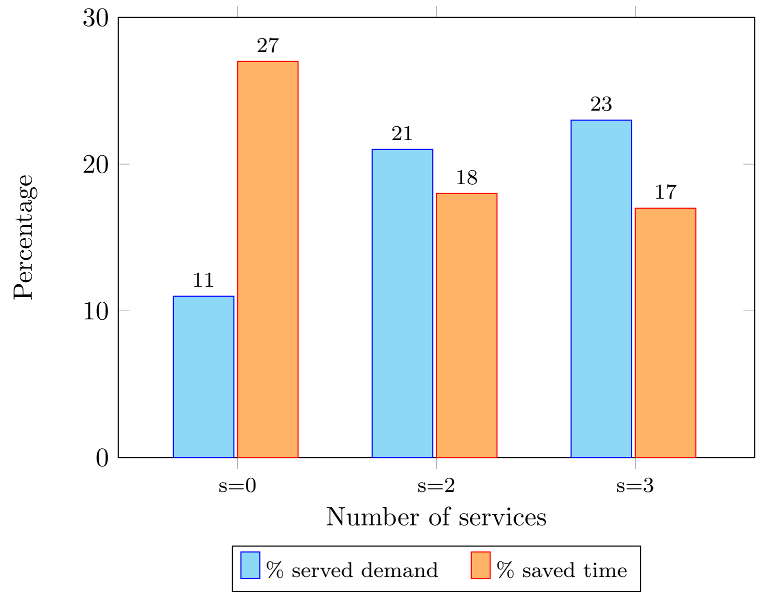

Figure 1: Effect of increasing the number of services: $n = 20 \mid p = 5 \mid r = 2.68 \mid \alpha = 0.5$

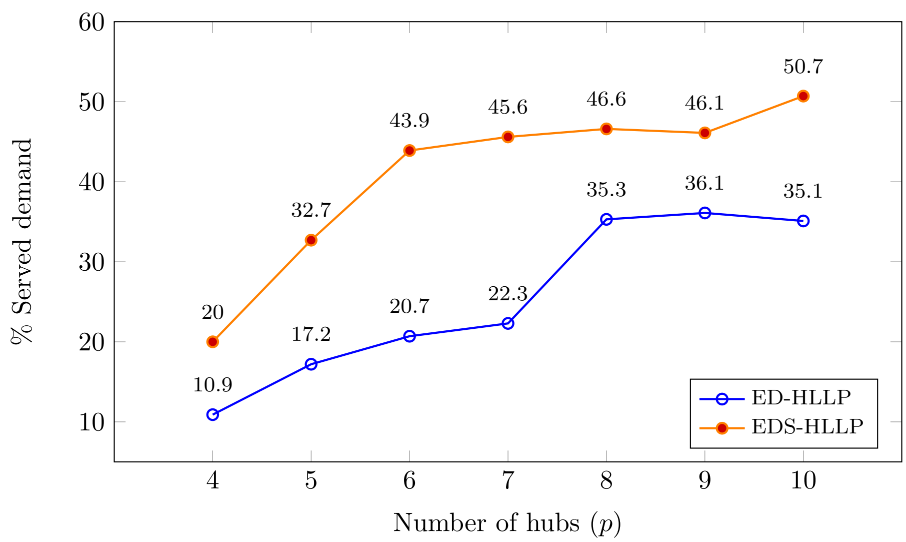

Figure 2: Impact of service integration on % served demand for varying values of p**.** $n = 15 \mid s = 3 \mid \alpha = 0.5 \mid r = 2.68$

Figure 3 compares the average of time saved in EDS-HLLP and ED-HLLP models; it shows how the saved time declines in both; however, our proposed model provides more consistent time savings compared with ED-HLLP, suggesting that the integration of services helps to maintain the efficiency of the hub line system even as the number of hubs increases.

5.3.4 Sensitivity to the weights of the demand model

Figure 4 depicts the effect of increasing the weight of Service 1 in the demand model (1). We can observe that increasing the weight of Service 1 six times (6x) from its original weight, the percentage of served demand increases from 32.7% to 39.6%, showing a remarkable increase in user attraction. However, this comes at the cost of time efficiency, as the saved time decreases from 20% to 16%, reflecting the trade-off between improving system attractiveness and maintaining time efficiency.

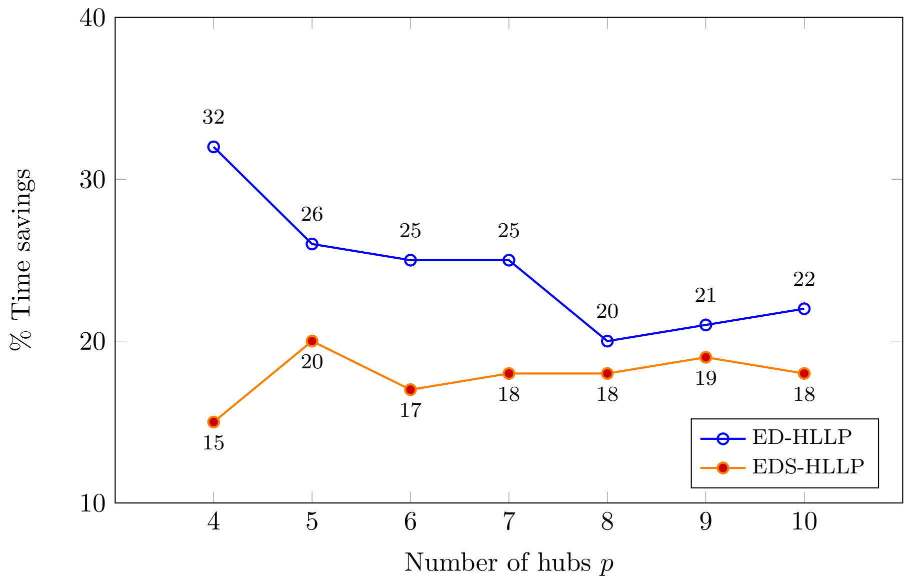

Figure 3: Impact of the service integration on % time savings for varying values of p. $n = 15 \mid s = 3 \mid \alpha = 0.5 \mid r = 2.68$

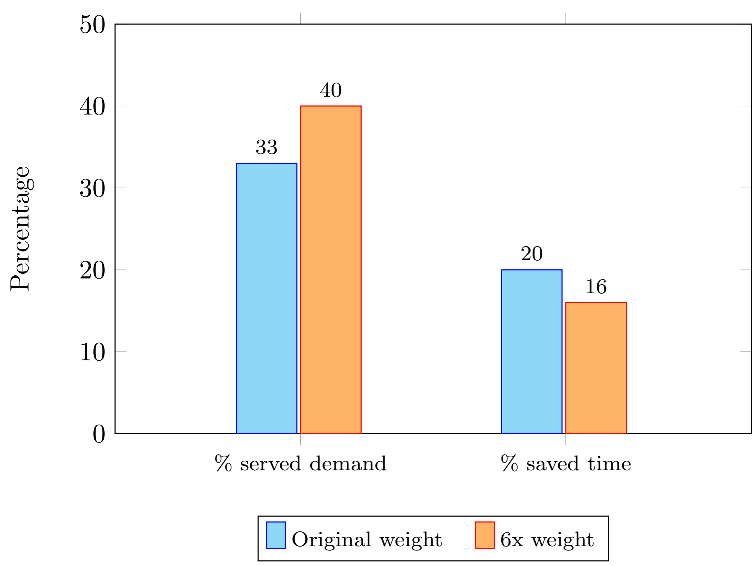

Figure 4: Effect of increasing the weight of Service 1: $n = 15 \mid p = 5 \mid s = 3 \mid B = 15 \mid \alpha = 0.5$

5.3.5 Sensitivity to the global budget B

Figure 5 shows, for $n = 20, p = 5, s = 2, \alpha = 0.5$ how sensitive our model is to the budget B. Without any restriction applied (i.e. by making $B = ps$), we observe that the percentage of served demand is on average of a 21%. Decreasing B to 5 triggers a significant reduction to only a 9%. The model compensates by providing higher time savings, as we observe from the improvement from a 18% to a 25%. These results suggest that while limiting the number of services could reduce the spatial distribution, it can also lead to higher time savings.

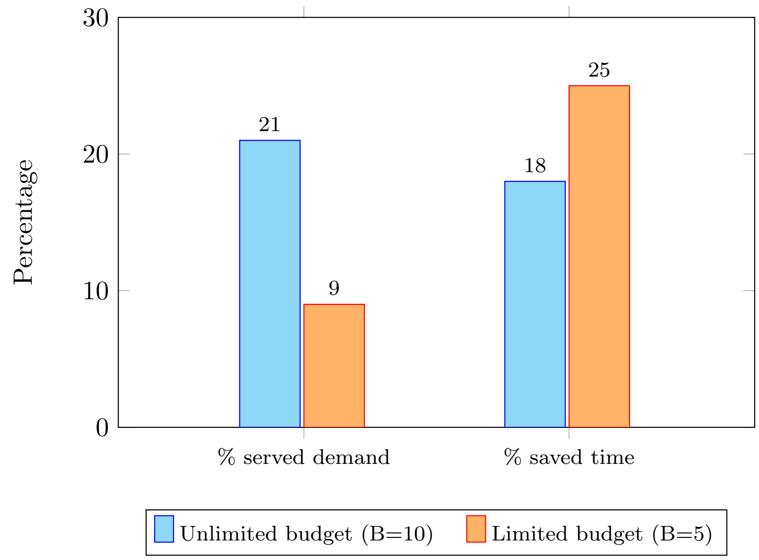

Figure 5: Effect of service restrictions: $n = 20 \mid p = 5 \mid s = 2 \mid B = 5, 10 \mid \alpha = 0.5$

5.3.6 Comparison of hub-line configurations

In our next analysis, we compare the hub selections, and line designs. Figures 6a and 6b show the hub lines obtained using the ED-HLLP proposed by Cobeña et al. (2023) model against our proposed model in this paper.

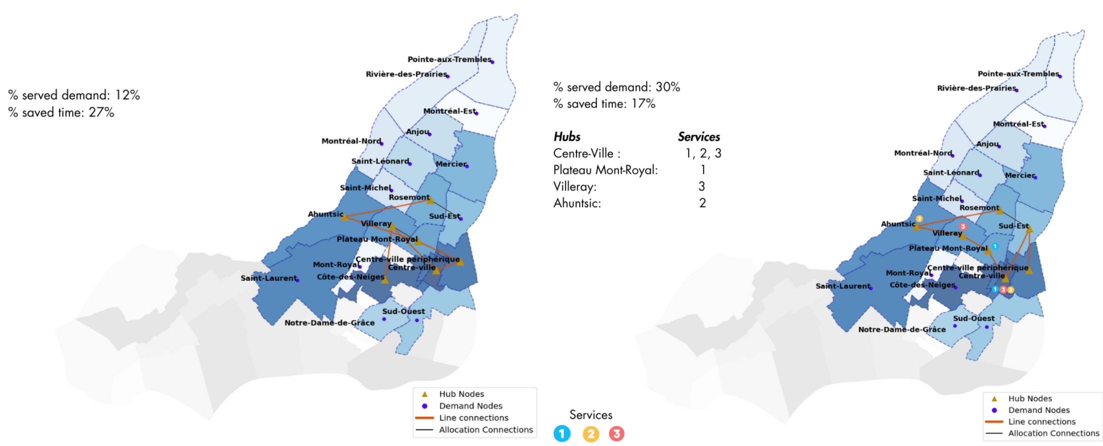

(a) ED-HLLP
$n = 20, p = 7, \alpha = 0.5, s = 0$

(b) EDS-HLLP
$n = 20, p = 7, \alpha = 0.5, s = 3, B = 7$

Figure 6: Hub-line configuration ED-HLLP vs EDS-HLLP

In Figure 6a, we see that some of the neighbourhoods chosen as hub nodes are “Plateau Mont-Royal”, “Côte-des-Neiges” and “Ahuntsic”, and the percentage of served demand is 12% with a 27% reduction in travel time. On the other hand, we can see in Figure 6b, incorporating three services $s = 3$ and a budget of $B = 7$, the proposed model improves significantly to 30% the percentage of demand indicating that a considered amount of the population benefits from the optimized hub-line configuration, experiencing a the reduction in travel times on average of a 17%.

We also observe now in Figure 6a which neighbourhoods are selected as hubs, in this case “Centre-Ville” —where services 1, 2 and 3 are offered— and “Plateau Mont-Royal” —where service number one is provided—. We can also observe in this case that in station *Centre-ville-Périphérique* our model suggests that is not necessary to provide services, reflecting the potential little advantage in terms of additional demand captured by the potential services that could be offered at that node.

Figures 7a and 7b serves at illustrating the type of hub-line configuration obtained when passing from $s = 2$ services per hub-node to $s = 3$ for an instance with $n = 20$, $p = 5$ and $\alpha = 0.5$, provided that the global budget for the installation of services are of $B = 5$ and $B = 10$, respectively.

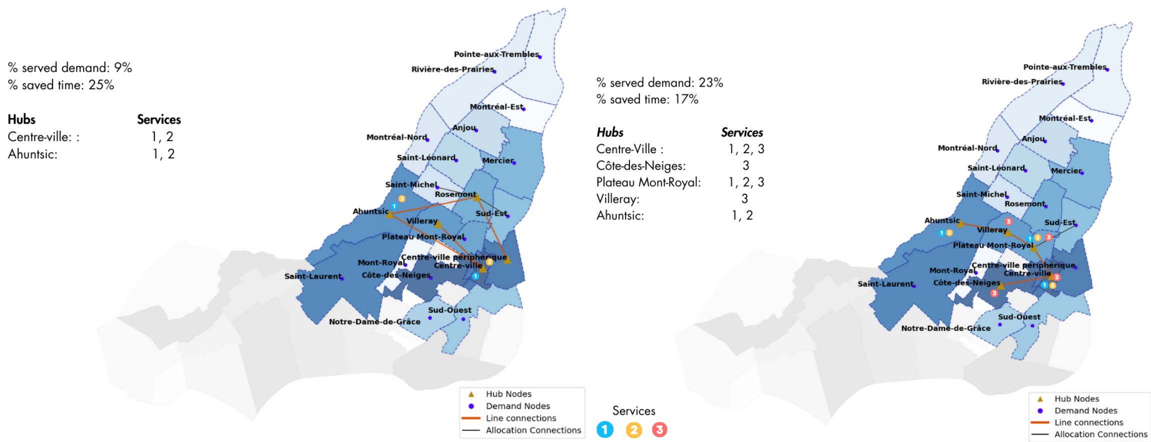

(a) $n = 20, p = 5, \alpha = 0.5, s = 2, B = 5$ **(b)** $n = 20, p = 5, \alpha = 0.5, s = 3, B = 10$

Figure 7: Configurations of the hub lines applying EDS-HLLP for $s = 2$ and $s = 3$

In Figure 7a, for $s = 2$, we observe that the neighbourhoods selected to locate hub-nodes are "Villeray", "Centre-Ville" and "Rosemont" among others, which serve 9% of the total demand with a 25% of time savings. In Figure 7b, when the number of services increases to $s = 3$, the hub-nodes now include "Côte-des-Neiges", "Plateau Mont-Royal" and 'Ahuntsic", among others, resulting in an increase of coverage to 23% for with a reduced time savings of only 17%. We observe, for instance, that in "Plateau Mont-Royal" and "Centre-Ville", services 1, 2 and 3 are offered.

Increasing the number of services s along with an increase in the global budgets B usually leads to an increase in the percentage of served demand and introduces some complexity that may affect the efficiency of the hub line network.

Overall, we can see how the attraction of the hub line system improves by applying our model, showcasing the importance of integrating the design of services with that of the hub-line networks.

6 Conclusions

In this paper we have introduced a novel approach to designing urban mobility hubs as a hub line network. The proposed model maximizes the the total profit experienced by the users traveling in the hub line network. Regarding demand elasticity, this work fills the gap in the literature of hub-line location problems by integrating service levels within the hub locations, adopting a simplified function to represent the path attractiveness. Finally, it relates to the the inclusion of service levels on mobility indicators such as spatial coverage and the saving times in the resulting hub line network.

The proposed model provides a flexible tool for decision-makers, especially when a large volume of data is available. It can be adjusted for various regions, areas, or cities; it can also serve as a comprehensive transportation model when neighbourhood-level data is utilized as a significant input for the model. This flexibility helps the model find the best locations for hubs by neighbourhood. It can serve as a decision support tool for city and transport planners who desire to design a new hub line network and mobility hubs with additional services.

The results reported in Section 5 highlight the critical importance of balancing the increasing service levels and maintaining time efficiency, as we observe that often these two performance indicators are inversely correlated. Another important observation raised from our study is that different neighbourhoods may profit from varying service needs. We observe how the integration of different levels of service result in changing design topologies. Overall, the proposed framework enables decision-makers to better address the mobility and varying needs of the urban populations.

From an algorithmic perspective, we observe that the proposed model can scale and solve quite large problems (with up to 39 potential hub-nodes), especially when the savings from the hub-line are moderate to low. On larger problems, or on problems with moderate to high time savings, the proposed model scales more poorly. This indicates that, from an algorithmic perspective, the proposed model could benefit from more elaborate methods, such as column generation (Cobeña and Contardo, 2024).

A Algorithm to create auxiliary directed graph G_c

The Algorithm 1 proposed by Cobeña et al. (2023) describes the procedure to create an auxiliary directed graph G_c that allows to build all possible paths between o_c and d_c using the hub line with an associated travel time smaller than or equal to $t_{o_c d_c}$.

Algorithm 1: Obtaining auxiliary graph $G_c = (N_c, A_c)$ and travel times t^c of each arc for $c \in C$.

Data: Graph $G = (N, E)$ with t_{ij} for $e = [i, j] \in E$ and $c \in C$.
Result: Auxiliary graph $G_c = (N_c, A_c)$ and t^c.

$N_c = N \cup \{o'_c, d'_c\}$.
A_c and t^c are generated as follows:
for $i, j \in N_c$ **do**
  if $i \neq j$ *and* $j \neq o_c$ *and* $i \neq d_c$ *and* $i \neq d'_c$ *and* $j \neq o'_c$ **then**
    if $t_{o_c i} + \tilde{t}^a_i + \alpha \cdot t_{ij} \leq t_{o_c d_c}$ **then**
      include (o_c, i) in A_c,
      $t^c_{o_c i} = t_{o_c i} + \tilde{t}^a_i$
    end
    if $\alpha \cdot t_{ij} + t_{j d_c} + \tilde{t}^e_j \leq t_{o_c d_c}$ **then**
      include (j, d_c) in A_c,
      $t^c_{j d_c} = t_{j d_c} + \tilde{t}^e_j$
    end
    if $\alpha \cdot t_{ij} \leq t_{o_c d_c}$ **then**
      include (i, j) in A_c,
      $t^c_{ij} = \alpha \cdot t_{ij}$
    end
  end
end
for $i \in N_c \setminus \{o_c, d_c, o'_c, d'_c\}$ **do**
  if *degree of i is smaller than or equal to 1* **then**
    $N_c = N_c \setminus \{i\}$
  end
end
return $G_c = (N_c, A_c)$ and t^c.

B Algorithm to generate all candidate paths

Algorithm 2 details the procedure to obtain all possible paths in a hub line composed by p hubs that Cobeña et al. (2023) proposed.

Algorithm 2: Obtaining all (ODH$_c$, DH$_c$, OH$_c$ and ODNH$_c$)-paths for a commodity $c \in C$.

Data: Graph $G = (N, E)$ with t_{ij} for $e = [i, j] \in E$ and $c \in C$.
Result: All possible (ODH$_c$, DH$_c$, OH$_c$ and ODNH$_c$)-paths for $c \in C$.
Build the auxiliary graph $G_c = (N_c, A_c)$ and travel times t^c by using Algorithm 1.
Search for the paths, π_c, associated to c (all_simple_paths$(G_c, o_c, d_c, p+1)$) such that:

$$\#\text{arcs}(\pi_c) \leq p + 1 \text{ and } \text{time}(\pi_c) \leq t_{o_c d_c}$$

.
Where $\#\text{arcs}(\pi_c)$ is the number of arcs in π_c and time(π_c) is the time of π_c.
Once a path π_c is obtained,
if *there exists an arc* (i, j) *of* π_c *such that* $t_{o_c i} + \tilde{t}_i^a + \alpha t_{ij} + \tilde{t}_j^e + t_{j d_c} \leq time(\pi_c)$ **then**
  remove π_c from the set of paths associated with (o_c, d_c).
end
Given a candidate path π_c, identify type of π_c:
if $i' = o_c$ *and* $j' = d_c$ **then**
  π_c is type ODH$_c$
end
if $i' = o_c$ *and* $j' \neq d_c$ **then**
  π_c is type OH$_c$
end
if $i' \neq o_c$ *and* $j' = d_c$ **then**
  π_c is type DH$_c$
end
if $i' \neq o_c$ *and* $j' \neq d_c$ **then**
  π_c is type ODNH$_c$
end
return All possible paths for c.

C Detailed computational results

This section presents detailed results of the proposed optimization method for different values of B. The first six columns for Tables 8–10 are used to report the characteristics of each problem, namely: i) the number of nodes in the problem (n); ii) the number of open hubs (p); iii) the number of services (s) to be offered, and iv) the total budget (B); v) the discount factor (α) used in the computation of the travel times using equation (3). The next nine columns are as follows: vi) column ($\mid \mathcal{P} \mid$) indicates the total number of paths enumerated; vii) column (t_{paths}) indicates the CPU time spent in the enumeration of the partial paths, this is the paths that ignore the provided services at the hub locations; viii) column (t_{post}) indicates the CPU time spent in the enumeration of the full paths, this is the paths that include the services at the entrance/egress points in each case; ix) column (t_{MIP}) indicates the CPU time spent in solving the MILP (7)–(22) to optimality; x) column (t_{tot}) corresponds to the sum of all the times; xi-xii) columns (**LB**)–(**UB**) indicate the final lower and upper bounds; and xiii) indicates the final relative gap, computed as $Gap = (UB - LB)/UB \times 100$.

Table 8: Performance of EDS-HLLP model with a budget of $B_1 = p * s$

n	p	s	B_1	α	$\mid \mathcal{P} \mid$	t_{paths}	t_{post}	t_{MIP}	t_{tot}	LB	UB	Gap
10	5	3	15	0.2	1362432	1.09	22.87	478.93	502.89	966120	966120	0.00
				0.5	22912	0.33	0.40	2.64	3.37	84857	84857	0.00
				0.8	3200	0.21	0.12	0.15	0.48	2619	2619	0.00
	7	3	21	0.2	5565184	11.81	146.67	72479.42	72637.90	1248449	1248449	0.00
				0.5	22912	4.63	0.47	6.37	11.47	107121	107121	0.00
				0.8	3200	3.36	0.17	2.66	6.18	2337	2337	0.00
15	5	3	15	0.2	17080448	36.05				mem		
				0.5	128768	7.66	2.25	24.30	34.21	100984	100984	0.00
				0.8	7808	3.01	0.34	0.48	3.83	2671	2671	0.00
	7	3	21	0.2				time				
				0.5	129152	604.87	2.36	61.84	669.07	133079	133079	0.00
				0.8	7808	239.49	0.39	8.16	248.03	2811	2811	0.00
20	5	3	15	0.2				time				
				0.5	429312	83.36	7.77	232.55	323.68	145816	145816	0.00
				0.8	14848	20.24	1.14	5.94	27.32	4368	4368	0.00
	7	3	21	0.2				time				
				0.5	432384	14356.49	8.03	436.35	14800.86	203382	203382	0.00
				0.8	14848	3930.42	1.19	19.92	3951.53	5287	5287	0.00
25	5	3	15	0.2				time				
				0.5	2569344	692.24	46.67	1436.18	2175.09	152903	152903	0.00
				0.8	26368	113.98	2.87	10.03	126.88	4014	4014	0.00
	7	3	21	0.2				time				
				0.5				time				
				0.8	26368	36416.79	2.69	22.76	36442.23	4610	4610	0.00
30	5	3	15	0.2				time				
				0.5	5427072	2854.49	97.70	7728.46	10680.64	164149	164149	0.00
				0.8	34944	334.75	5.94	8.37	349.06	3835	3835	0.00
	7	3	21	0.2				time				
				0.5				time				
				0.8				time				
39	5	3	15	0.2				time				
				0.5				time				
				0.8	90112	2090.89	15.59	30.70	2137.19	3548	3548	0.00
	7	3	21	0.2				time				
				0.5				time				
				0.8				time				

Table 9: Performance of EDS-HLLP model with a budget of $B_2 = 2/3(p * s)$

n	p	s	B_2	α	$\mid \mathcal{P} \mid$	t_{paths}	t_{post}	t_{MIP}	t_{tot}	LB	UB	Gap
10				0.2	1362432	1.09	22.90	6430.53	6454.51	797101	797101	0.00
	5	3	10	0.5	22912	0.33	0.41	24.09	24.82	70342	70342	0.00
				0.8	3200	0.21	0.12	1.13	1.45	2302	2302	0.00
				0.2	5565184	11.81	98.14	86409.83	86519.78	987610	1339123	26.25
	7	3	14	0.5	22912	4.63	0.48	163.58	168.69	92142	92142	0.00
				0.8	3200	3.36	0.17	6.60	10.13	2119	2119	0.00
15				0.2	17080448	36.05				mem		
	5	3	10	0.5	128768	7.66	2.27	158.68	168.61	85321	85321	0.00
				0.8	7808	3.01	0.33	2.41	5.76	2268	2268	0.00
				0.2				time				
	7	3	14	0.5	129152	604.87	1.36	1003.75	1609.98	114764	114764	0.00
				0.8	7808	239.49	0.33	45.08	284.89	2581	2581	0.00
20				0.2				time				
	5	3	10	0.5	429312	83.36	8.06	1547.67	1639.08	125275	125275	0.00
				0.8	14848	20.24	1.14	31.33	52.72	3888	3888	0.00
				0.2				time				
	7	3	14	0.5	432384	14356.49	8.34	61682.53	76047.35	173439	173439	0.00
				0.8	14848	3930.42	1.13	108.94	4040.49	4746	4746	0.00
25				0.2				time				
	5	3	10	0.5	2569344	692.24	43.99	69122.38	69858.62	130616	130616	0.00
				0.8	26368	113.98	2.86	56.91	173.75	3408	3408	0.00
				0.2				time				
	7	3	14	0.5				time				
				0.8	26368	36416.79	2.84	213.84	36633.47	4183	4183	0.00
30				0.2				time				
	5	3	10	0.5	5427072	2854.49	95.93	64260.41	67210.83	144378	144378	0.00
				0.8	34944	334.75	6.02	144.21	484.99	3311	3311	0.00
				0.2				time				
	7	3	14	0.5				time				
				0.8				time				
39				0.2				time				
	5	3	10	0.5				time				
				0.8	90112	2090.89	15.48	113.86	2220.23	3145	3145	0.00
				0.2				time				
	7	3	14	0.5				time				
				0.8				time				

Table 10: Performance of EDS-HLLP model with a budget of $B_3 = 1/3(p * s)$

n	p	s	B_3	α	$\mid \mathcal{P} \mid$	t_{paths}	t_{post}	t_{MIP}	t_{tot}	LB	UB	Gap
10				0.2	1362432	1.09	25.22	8560.89	8587.19	551482	551482	0.00
	5	3	5	0.5	22912	0.33	0.56	26.83	27.71	49851	49851	0.00
				0.8	3200	0.21	0.12	4.19	4.52	1535	1535	0.00
				0.2	5565184	11.81	96.28	260.69	86406.54	719611	909238	20.86
	7	3	7	0.5	22912	4.63	0.45	765.98	771.06	64411	64411	0.00
				0.8	3200	3.36	0.12	6.61	10.09	1679	1679	0.00
15				0.2	17080448	36.05			mem			
	5	3	5	0.5	128768	7.66	2.59	161.18	171.43	63191	63191	0.00
				0.8	7808	3.01	0.35	5.23	8.58	1707	1707	0.00
				0.2				time				
	7	3	7	0.5	129152	604.87	1.29	601.03	1207.19	85543	85543	0.00
				0.8	7808	239.49	0.21	15.04	254.74	1974	1974	0.00
20				0.2				time				
	5	3	5	0.5	429312	83.36	7.70	4095.73	4186.78	87246	87246	0.00
				0.8	14848	20.24	1.01	75.38	96.63	2758	2758	0.00
				0.2				time				
	7	3	7	0.5	432384	14356.49	4.42	29350.50	43711.41	128526	128526	0.00
				0.8	14848	3930.42	0.59	118.30	4049.31	3501	3501	0.00
25				0.2				time				
	5	3	5	0.5	2569344	692.24	44.76	58026.54	58763.54	90761	90761	0.00
				0.8	26368	113.98	2.83	74.21	191.02	2590	2590	0.00
				0.2				time				
	7	3	7	0.5				time				
				0.8	26368	36416.79	1.56	393.17	36811.52	3179	3179	0.00
30				0.2				time				
	5	3	5	0.5	5427072	2854.49	96.52	66347.56	69298.56	96880	96880	0.00
				0.8	34944	334.75	6.07	194.33	535.15	2450	2450	0.00
				0.2				time				
	7	3	7	0.5				time				
				0.8				time				
39				0.2				time				
	5	3	5	0.5				time				
				0.8	90112	2090.89	15.63	390.51	2497.03	2286	2286	0.00
				0.2				time				
	7	3	7	0.5				time				
				0.8				time				

References

A. Schäfer, Long-term trends in global passenger mobility, in: Frontiers of Engineering: Reports on Leading-Edge Engineering from the 2006 Symposium, National Academies Press, 2007, p. 85.

UN, World urbanization prospects 2018, 2009.

N. Aydin, S. Seker, B. Özkan, Planning location of mobility hub for sustainable urban mobility, Sustainable Cities and Society 81 (2022) 103843.

Metrolink, Mobility hub guidelines: For the greater toronto and hamilton area, 2011b. URL: http://www.metrolinx.com/en/regionalplanning/mobilityhubs/MobilityHubGuidelines.pdf.

T. Arnold, M. Frost, A. Timmis, S. Dale, S. Ison, Mobility hubs: review and future research direction, Transportation Research Record 2677 (2023) 858–868.

R. Z. Farahani, M. Hekmatfar, A. B. Arabani, E. Nikbakhsh, Hub location problems: A review of models, classification, solution techniques, and applications, Computers and Industrial Engineering 64 (2013) 1096–1109.

S. A. Alumur, J. F. Campbell, I. Contreras, B. Y. Kara, V. Marianov, M. E. O'Kelly, Perspectives on modeling hub location problems, European Journal of Operational Research 291 (2021) 1–17.

B. Cobeña, I. Contreras, L. I. M. Merino, A. M. Rodríguez-Chía, The profit-oriented hub line location problem with elastic demand, Computers & Operations Research (2023) 106335.

S. Aono, Identifying Best Practices for Mobility Hubs, TransLink, 2019.

SANDAG, Mobility hub features catalog, 2017. URL: http://www.sdforward.com/fwddoc/mobipdfs/mobilityhubcatalog-features.pdf.

R. Nair, E. Miller-Hooks, Equilibrium network design of shared-vehicle systems, European Journal of Operational Research 235 (2014) 47–61.

K. Steiner, S. Irnich, Strategic planning for integrated mobility-on-demand and urban public bus networks, Transportation Science 54 (2020) 1616–1639.

L. Caggiani, A. Colovic, M. Ottomanelli, An equality-based model for bike-sharing stations location in bicycle-public transport multimodal mobility, Transportation Research Part A: Policy and Practice 140 (2020) 251–265.

L. Frank, N. Dirks, G. Walther, Improving rural accessibility by locating multimodal mobility hubs, Journal of Transport Geography 94 (2021) 103111.

S. Xanthopoulos, M. van der Tuin, S. S. Azadeh, G. H. de Almeida Correia, N. van Oort, M. Snelder, Optimization of the location and capacity of shared multimodal mobility hubs to maximize travel utility in urban areas, Transportation Research Part A: Policy and Practice 179 (2024) 103934.

V. Stadnichuk, L. Merten, C. Larisch, G. Walther, Optimisation of mobility hub locations for a sustainable mobility system, Transportation Research Interdisciplinary Perspectives 26 (2024) 101193.

E. Martins de Sá, I. Contreras, J.-F. Cordeau, R. Saraiva de Camargo, G. de Miranda, The hub line location problem, Transportation Science 49 (2015) 500–518.

T. Drezner, Z. Drezner, A note on applying the gravity rule to the airline hub problem, Journal of Regional Science 41 (2001) 67–72.

H. A. Eiselt, V. Marianov, A conditional p-hub location problem with attraction functions, Computers & Operations Research 36 (2009) 3128–3135.

H. A. Eiselt, G. Laporte, Demand allocation functions, Location Science 6 (1998) 175–187.

G. Laporte, J. A. Mesa, F. A. Ortega, Locating stations on rapid transit lines, Computers & Operations Research 29 (2002) 741–759.

T. Drezner, Z. Drezner, Validating the gravity-based competitive location model using inferred attractiveness, Annals of Operations Research 111 (2002) 227–237.

T. Drezner, Z. Drezner, Finding the optimal solution to the huff based competitive location model, Computational Management Science 1 (2004) 193–208.

T. Drezner, Z. Drezner, Multiple facilities location in the plane using the gravity model, Geographical Analysis 38 (2006) 391–406.

T. Drezner, Z. Drezner, The gravity p-median model, European Journal of Operational Research 179 (2007) 1239–1251.

G. Erdoğan, J.-F. Cordeau, G. Laporte, The attractive traveling salesman problem, European Journal of Operational Research 203 (2010) 59–69.

C. A. Zetina, I. Contreras, J. Cordeau, Profit-oriented fixed-charge network design with elastic demand, Transportation Research Part B: Methodological 127 (2019) 1–19.

B. Cobeña, C. Contardo, Column generation for the profit-oriented hub-line location problem with elastic demands, Les Cahiers du GERAD G-2024-58, Groupe d'études et de recherche en analyse des décisions, GERAD, Montréal QC H3T 2A7, Canada, 2024. URL: https://www.gerad.ca/en/papers/G-2024-58. arXiv:https://www.gerad.ca/papers/G-2024-58.pdf?locale=en.

T. Sonesson, Inter-urban travel demand elasticities with emphasis on trip generation and destination substitution, Journal of Transport Economics and Policy (JTEP) 35 (2001) 301–326.

S. Goh, K. Lee, J. S. Park, M. Choi, Modification of the gravity model and application to the metropolitan seoul subway system, Physical Review E 86 (2012) 026102.

E. Martins de Sá, I. Contreras, J.-F. Cordeau, R. De Camargo, G. De Miranda, The hub line location problem, Transportation Science 49 (2015) 500–518.